Elektrotehniški vestnik 73(1): 25-30, 2006
Electrotechnical Review: Ljubljana, Slovenija

Electrical Drive Inductive Coupling

Irena Kováčová[1], Dobroslav Kováč[2]

[1] *Department of Electrical Drives and Mechatronics, Technical University of Košice, Letná 9, 042 00 Košice, Slovak Republic*
[2] *Department of Theoretical Electrotechnics and Electrical Measurement, Park Komenského 3, 042 00 Košice, Slovak Republic*
E-mail: Irena.Kovacova@tuke.sk, Dobroslav.Kovac@tuke.sk

Abstract The paper presents a computer analysis of inductive coupling of the electromagnetic compatibility (EMC) problem. Its focus is on power electronics and electrical drives and tests performed by a numerical computer simulation that can disclose suite surprising findings about EMC problems.

Keywords: electromagnetic compatibility, power electronics, converters, inverters.

1 Introduction

Importance of electromagnetic compatibility (EMC) of all electrical products has been rapidly growing during the last decade. The environment is increasingly polluted by electromagnetic energy. The interference impact on the surroundings is being doubled every three years and covers a large frequency range.

Equipment disturbances and errors have become more serious as a consequence of the growth of the electronic circuit complexity. According to new technical legislation and also economic consequences, the EMC concept of all products must be strictly observed [1]. It must start with the specification of the equipment performance and end with the equipment installation procedures.

2 EMC and environmental waste

We all know the environmental pollution problems caused by solid, liquid and gaseous wastes. We are aware of most of these pollutants through our senses.
Due to the increasing life standard, contamination of our environment by the electromagnetic energy is constantly increasing too. Since human beings have no organs for perception of such contamination, they cannot perceive it. The great producers of such waste are electronic systems developed by man and meant to be effective within these electromagnetic surroundings producing, of course, electromagnetic waste in turn [2].

On one side, interferences are deliberately or involuntarily produced. The place of their origin is called interference source. On the other side, devices may be hindered in their function by such interferences. Those objects are called interference objects.

The possible interfaces between sources and objects are shown in Fig. 1. There are four basic types of coupling that can realize these interfaces.

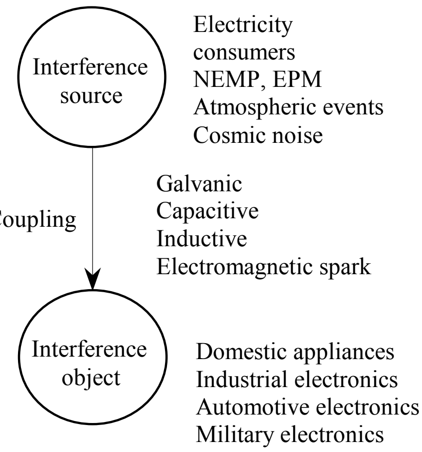

Fig. 1. Interference diagram

3 EMC – the interference mechanism

The interference mechanism can be described in a simplified form as follows. The interference source can be for instance a power semiconductor converter or motor. Interference is produced in the interference source getting into electronics in undesirable ways and is due to various effects distorting signals. Transmission can be direct, for example by galvanic coupling between interference source and interference sink. Interference can be spread through air or via ducts, or coupled inductively or capacitively into signal lines [3].

Received 8. March, 2005
Accepted 25. March, 2005

Development of power semiconductor elements has caused vehement evolution of the power electronics branch in the last ten years. To investigate the converter functionality, it was necessary first to theoretically analyze and then practically verify its assumed activity. Now, we can eliminate the laborious theoretical analysis by a numerical computer simulation, which can disclose quite surprising findings about EMC [4].

4 Inductive coupling

Inductive coupling is typical for two and more galvanically separated electric loops at the moment when the smaller one is driven by a time variable-current creating the corresponding, time-variable magnetic field [5]. In such case their mutual intercircuit effect is expressed as a function of the slope of the current increase or decrease, circuit environmental magnetic property as well as circuit geometric dimensions.

To predict the intercircuit inductive coupling, our focus will be on two electric loops l_1 and l_2 with currents i_1 and i_2. We will try to determine the effect of loop l_1 on loop l_2 (Fig. 2).

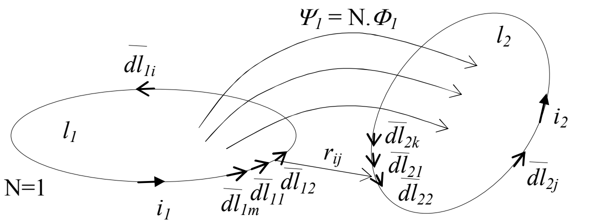

Fig. 2. Investigated loops

According to the Maxwell's equation for a quasi-stationary magnetic field

$$rot\,\overline{E} = -\frac{\partial \overline{B}}{\partial t} \tag{1}$$

and following its integral form

$$\int_S rot\,\overline{E}.d\overline{S} = -\int_S \frac{\partial \overline{B}}{\partial t}.d\overline{S} = -\frac{\partial}{\partial t}\int_S \overline{B}.d\overline{S} \tag{2}$$

and after applying the Stoke's theorem, we obtain the equation for the induced voltage [6];

$$u_{i2} = -\mathrm{N}.\frac{\partial \phi_1}{\partial t} = -\frac{\partial \psi_1}{\partial t} = -M\,\frac{\partial i_1}{\partial t} \tag{3}$$

where M is the coefficient of the mutual inductance. For the magnetic flux Ψ_1 definition the equation

$$\phi_1 = \oint_{l_2} \overline{A}_2.d\overline{l}_2 \tag{4}$$

is valid where $\overline{A}_2$ is the vector of the magnetic field potential created by the current i_1. We can calculate the value of this vector by the following equation:

$$\overline{A}_2 = \frac{\mu.i_1}{4\pi}\oint_{l_1}\frac{d\overline{l}_1}{r_{12}}. \tag{5}$$

After substituting the last equation with the equation valid for the magnetic flux ϕ_1, the next relation is obtained:

$$\phi_1 = \oint_{l_2}\left[\frac{\mu.i_1}{4\pi}\oint_{l_1}\frac{d\overline{l}_1}{r_{12}}\right].d\overline{l}_2 = \frac{\mu.i_1}{4\pi}\oint_{l_1}\oint_{l_2}\frac{d\overline{l}_1.d\overline{l}_2}{r_{12}} \tag{6}$$

and then

$$u_{i2} = -\frac{\partial\left(\dfrac{\mu.i_1}{4\pi}\oint_{l_1}\oint_{l_2}\dfrac{d\overline{l}_1.d\overline{l}_2}{r_{12}}\right)}{\partial t} = -\frac{\left(\dfrac{\mu}{4\pi}\oint_{l_1}\oint_{l_2}\dfrac{d\overline{l}_1.d\overline{l}_2}{r_{12}}\right)\partial i_1}{\partial t} = -M\frac{\partial i_1}{\partial t}. \tag{7}$$

For the practical use, it is more advantageous to express the induced voltage in the form of a differential:

$$u_i = -\frac{di}{dt}.\sum_{i=1}^{m}\sum_{j=1}^{k}\frac{\mu}{4\pi}\frac{dl_{1i}.dl_{2j}.\cos\gamma_{dlij}}{r_{ij}}. \tag{8}$$

If we know the geometrical dimensions of the investigated loops (Fig. 3) and want to determine their mutual inductive coupling then we can use the next relation (9) for the induced voltage. It is based on the 3D Cartesian coordinate system.

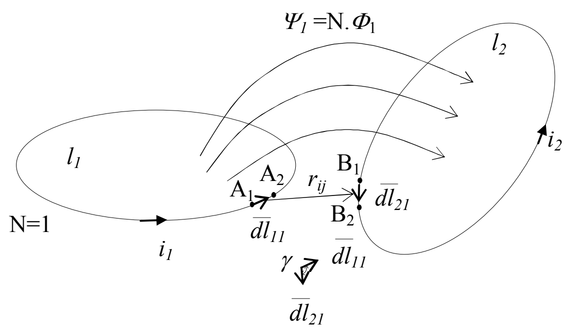

Fig. 3. Geometric dimensions of the investigated loops

$$u_i = -\frac{di}{dt}.\sum_{i=1}^{m}\sum_{j=1}^{k}\frac{\mu}{4\pi}\frac{(A_{x2i}-A_{x1i}).(B_{x2j}-B_{x1j})+(A_{y2i}-A_{y1i}).(B_{y2j}-B_{y1j})+(A_{z2i}-A_{z1i}).(B_{z2j}-B_{z1j})}{\sqrt{\left(\left(B_{x1j}+\frac{|B_{x2j}-B_{x1j}|}{2}\right)-\left(A_{x1i}+\frac{|A_{x2i}-A_{x1i}|}{2}\right)\right)^2+\left(\left(B_{y1j}+\frac{|B_{y2j}-B_{y1j}|}{2}\right)-\left(A_{y1i}+\frac{|A_{y2i}-A_{y1i}|}{2}\right)\right)^2+\left(\left(B_{z1j}+\frac{|B_{z2j}-B_{z1j}|}{2}\right)-\left(A_{z1i}+\frac{|A_{z2i}-A_{z1i}|}{2}\right)\right)^2}} \tag{9}$$

For a global solution of the inductive coupling part of the EMC problem inside the overall electric power system, it is necessary to analyze the circuit globally paying due regard to the mutual intercircuit inductance coupling. The result is the following integral-differential system of equations:

$$u_{cc1} = R_{c1}.i_1 + L_{c1}.\frac{di_1}{dt} + \frac{1}{C_{c1}}\int i_1.dt + \sum_{\substack{j=1 \\ j\neq 1}}^{k} u_{ij} \tag{10}$$

.
.
.

$$u_{cck} = R_{ck}.i_k + L_{ck}.\frac{di_k}{dt} + \frac{1}{C_{ck}}\int i_k.dt + \sum_{\substack{j=1 \\ j\neq k}}^{k} u_{ij} \tag{11}$$

For this purpose it is very suitable to explore the existing simulation programs such as for instance the PSPICE program utilized worldwide.

In the next part, we will try to determine the effect of the one-quadrant impulse converter on the sensing circuit as it shown in Fig. 4. The circuit dimensions are a = 0.2 m, b = 0.3 m, c = 0.1 m, d = 0.05 m, e = 0.005m. The radius of the copper wires is R = 0.0006 m and the relative permitivity of the circuit environment is μ_r = 0.991.

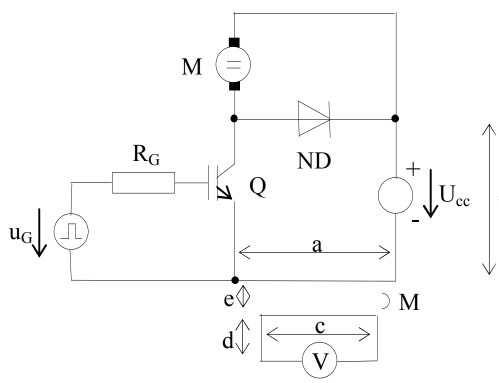

Fig. 4. Investigated circuit

The inductance of the first loop is given as

$$L_1 = L_{e1} + L_{i1} = \frac{\mu_0 b}{\pi}\ln\frac{a-R}{R} + \frac{\mu_0 a}{\pi}\ln\frac{b-R}{R} + \frac{\mu.2.(a+b)}{8\pi} = 1.294\mu H \tag{12}$$

and of the second as

$$L_2 = L_{e2} + L_{i2} = \frac{\mu_0 c}{\pi}\ln\frac{d-R}{R} + \frac{\mu_0 d}{\pi}\ln\frac{c-R}{R} + \frac{\mu.2.(c+d)}{8\pi} = 0.294\mu H \tag{13}$$

The mutual inductance M calculated from the above mentioned equation is M = 477.4 nH. The magnetic coupling coefficient k is given as

$$k = \frac{M}{\sqrt{L_1 + L_2}} = 0.774. \tag{14}$$

Now we can use the PSPICE simulation program for solving the inductive coupling problem between the two circuits [7]. Parameters of the circuit simulation are R_Z = 11.66 Ω, L_Z = 400 μH, R = 10 Ω, R_G = 100 Ω and U_{CC} = 70V. The schematic connection is shown in Fig. 5. The IGBT transistor Q was switched on at the frequency 10 kHz and the switch on/off ratio was 0.5.

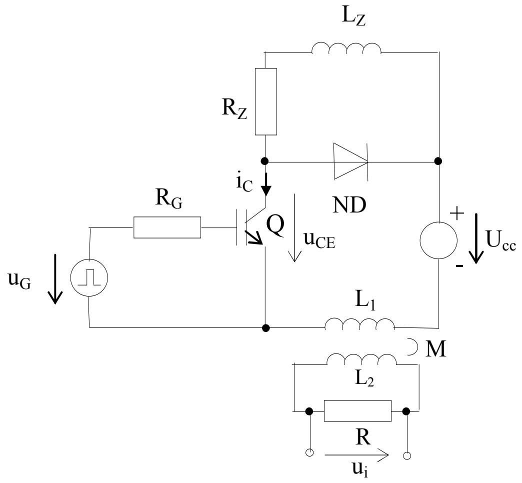

Fig. 5. Simulation circuit

Simulation results are shown in Fig. 6. Results obtained with measurements are shown in Figs. 7 and 8 and switching details in Figs. 9 and 10.

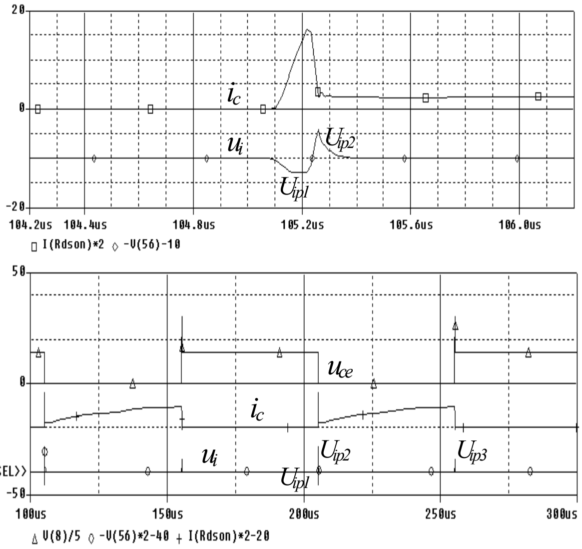

Fig. 6. Simulation results

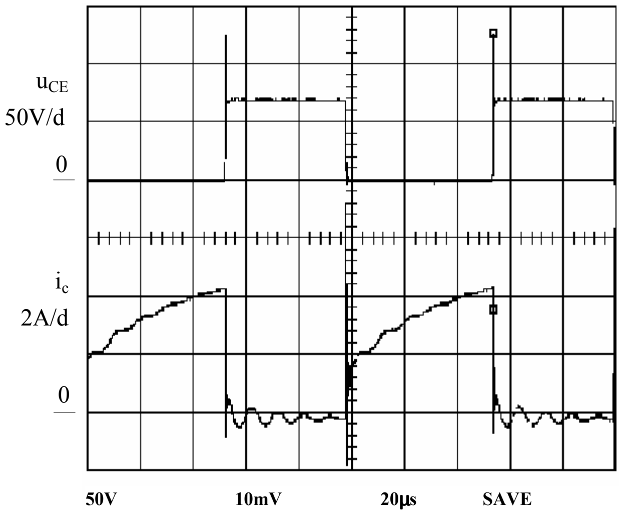

Fig. 7. Measured voltage u_{CE} and current i_C

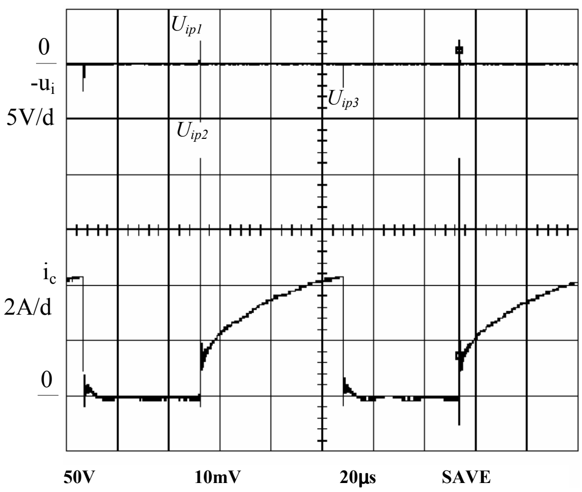

Fig. 8. Measured voltage $-u_i$ and current i_C

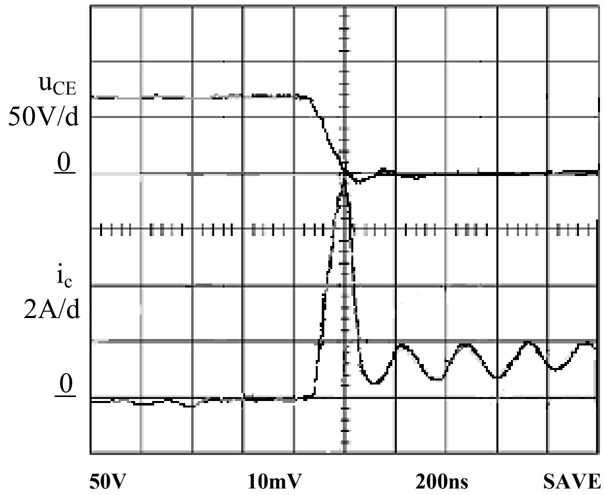

Fig. 9. Switching on voltage u_{CE} and current i_C

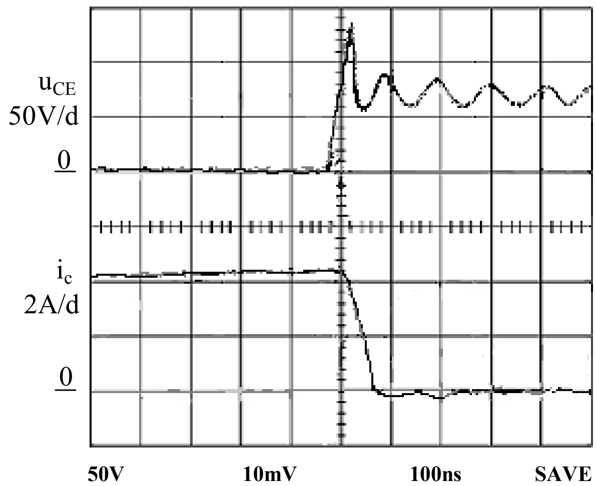

Fig. 10. Switching off voltage u_{CE} and current i_C

A comparison of the simulated and measured results shows that peaks of transistor current ic have the same values, i.e. 8.4 A, in both cases. The same values, i.e. 4.4 A, have both the simulated and measured transistor current at the moment when transistor is switched off. There is a small difference only between the simulated and measured curves of the transistor voltage uCE. The overvoltage generated at the transistor switching off reaches the value of 150 V for the simulated result. However, the corresponding overvoltage has only the value of 130 V for the measured result. Peaks of the simulated and measured induced voltages have the same values of Ui1 = -2.2V, Ui2 = 5.02V, Ui1 = 2.1V. This means that such method is acceptable for inductive coupling investigation of the EMC problem.

To improve the obtained results, the numerical solution of the magnetic field by finite element method program was also used. The result of such analysis is shown in Fig. 11.

From the "integral result" data window it is seen, that the value of the magnetic flux inside the sensing circuit is $3.317.10^{-9}$ Wb. Based on the basic program property allowing semi-real 3D space simulation with the 3rd dimension equal only to the basic unit of the depth (1mm), we multiplied the obtained value of the magnetic flux by the value of the sensing circuit depth c = 100 mm. The total magnetic flux was then $331.7.10^{-9}$ Wb. This flux was excited by the peak circuit current 8.4 A, the rising time of which was 120 ns. On the basis of the above equations, the first peak of the induced voltage can be calculated as

$$U_{ip1} = \frac{\Delta\Phi_1}{\Delta t_1} = \frac{0 - 331.7.10^{-9}}{140.10^{-9}} = \frac{-331{,}7.10^{-9}}{140.10^{-9}} = -2.369\ \mathrm{V}\,. \tag{15}$$

Similarly, it is possible to calculate the rest of the peaks of the induced voltage u_i:

$$U_{ip2} = \frac{\Delta\Phi_2}{\Delta t_2} = \frac{331.7.10^{-9} - 55.3.10^{-9}}{55.10^{-9}} = \frac{276.4.10^{-9}}{55.10^{-9}} = 5.025\mathrm{V} \tag{16}$$

$$U_{ip3} = \frac{\Delta\Phi_3}{\Delta t_3} = \frac{173.7.10^{-9} - 0}{80.10^{-9}} = \frac{173.7.10^{-9}}{80.10^{-9}} = 2.171\ \mathrm{V}\,. \tag{17}$$

The results obtained by the finite element numerical simulation method are again confirming the correctness of the above mentioned methods.

5 Conclusion

The performed analyses indicate that the fast power field effect transistor switching can produce the induced voltage with the value of some volts up to some tenths' of volts in the nearby circuits. It is also evident that the magnitude of the induced voltage depends on the magnetic flux slope. This means that fast switching of small currents can generate large peaks of the induced voltage, too.

6 References

[1] V. Kůs, „Influence of semiconductor converters on feeding distribution net", BEN Publishing, Praha, 2002

[2] P. Vaculíková, „Electromagnetic Compatibility of Electrical Engineering Systems", Grada Publi-shing, Praha 1998.

[3] K. Kováč, A. Lenková, „Electromagnetic Compa-tibility," Bratislava 1999.

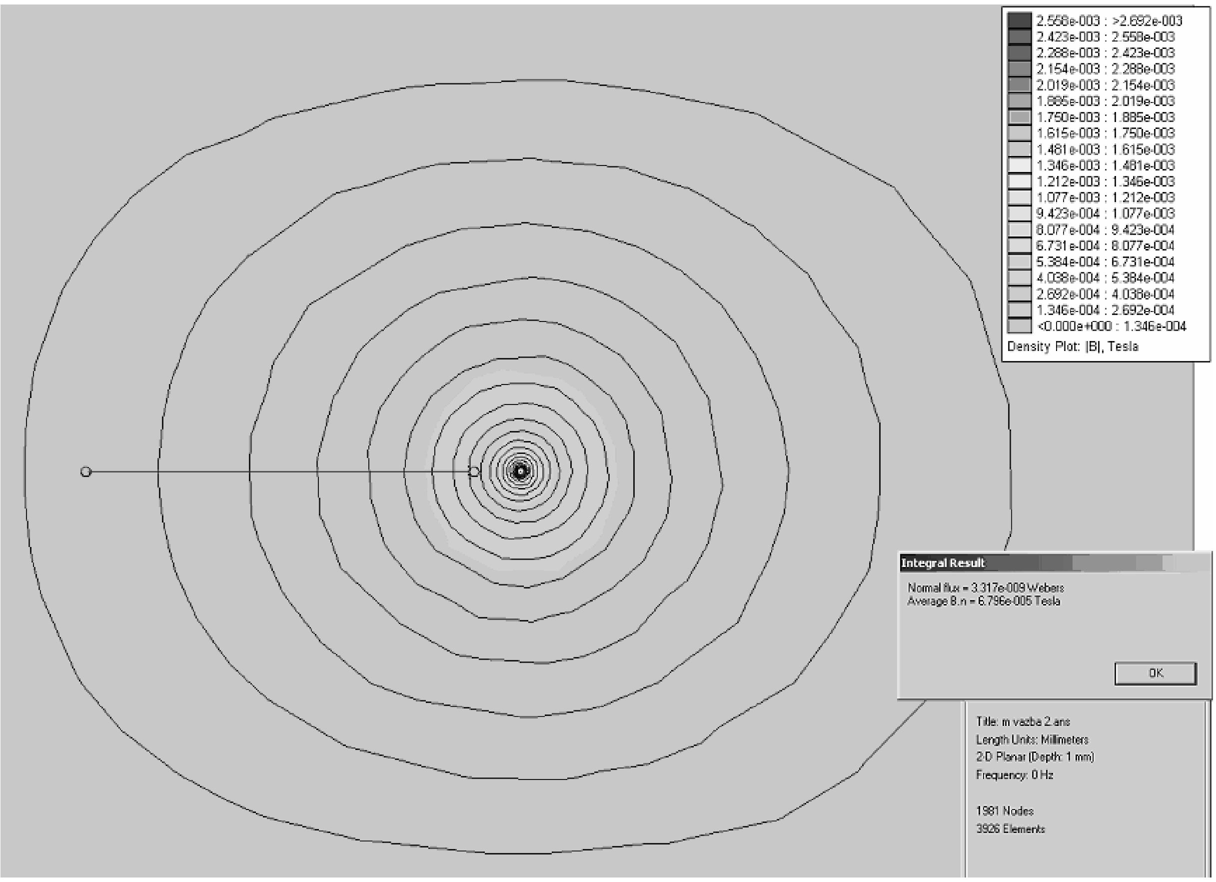

Fig. 11. The finite element simulation method of the magnetic field

[4] V. Šimko, I. Kováčová, „Transient actions in impulse converters with DC voltage feeding circuit”, Theoretical Electrical Engineering at Technical Universities, West Bohemian Univer-sity Plzeň, No. 4, 1994, pp. 91-96.
[5] I. Kováčová, J. Kaňuch, D. Kováč „Electromag-netic compatibility of electric power systems”, EQUILIBRIA Publishing, Košice, 2005.
[6] V. Šimko, D. Kováč, I. Kováčová, „Theoretical Electrical Engineering I.”, Elfa s.r.o. Publishing, Košice, 2002.
[7] D. Kováč, I. Kováčová, „Effect of Utilizing Static Power Semiconductor Converters on Quality of Electric Power Line Parameters,” Quality Innovation Prosperity, 2001, No. 1, pp. 74-84.
[8] J. Kaňuch, „Investigation methodology design of EMC for drives with disc motor.” Dissertation thesis, FEI TU Košice, 2005.
[9] Š. Gallová, „Numerical Control Programming Approach.” Transactions of the Universities of Košice, No. 1, 2004, pp. 48-52.
[10] D. Mayer, B. Ulrych, M. Škopek, „Electro-magnetic Field Analysis by Modern Software Products.” Journal of Eletrical Engineering, Vol. 7, No.1, 2001.
[11] D. Kudelas, R. Rybár, „Pneumatic - accumulated system enabling of small potential winding energy utilizing for electrical energy supplying.” AT&P Journal, Bratislava, No. 5, 2005, pp. 113-114.
[12] Š. Gallová, „Numerical Control Programming Approach.” Transactions of the Universities of Košice, No. 1, 2004, pp. 48-52.
[13] I. Kováčová, „EMC of Power DC Electrical Drives", Journal of Electrical Engineering, Romania, Vol. 5, No.1, 2005, pp. 61-66.
[14] I. Kováčová, J. Kaňuch, D. Kováč, „DC per-manent magnet disc motor design with improved EMC“, Acta Technica CSAV, Vol. 50, No.3, 2005, pp.291-306.
[15] I. Kováčová, J. Kaňuch, D. Kováč, „The EMC of Electrical Systems - Galvanic Coupling (Part I.)”, Acta Electrotechnica et Informatica, 2005, Vol.5, pp.22-28.

7 Acknowledgement

The paper has been prepared by the support of the Slovak grant projects No.1/0376/2003 and No. 1/1084/2004 and 1/1084/04.

Kováčová Irena - graduated in 1982 from the Technical University of Košice. From then on she has been employed with the Department of Electrical Drives at the same university first as an assistant lecturer and now as an associate professor. In 1988 she received her Ph.D. degree. In 1991 she was awarded from the Minister of Education for Development of Science and Technology. Her working interest is mainly in the field of power electronics, especially in construction of converters and inverters with new perspective elements and computer simulation of new power semiconductor parts and devices.

Kováč Dobroslav - graduated in 1985 from the Technical University of Košice. He then worked as a researcher at the Department of Electrical Drives at the same university. His research work at this time was focused on practical applications of new power semiconductor devices. In 1989 he received the award by the Minister of Education for Development of Science and Technology. From 1991-2000 was an assistant lecturer at the Department of Theoretical Electrical Engineering and Electric Measurement. He received his Ph.D. degree in 1992 for the work in the field of power electronics. From 2000 onwards he has worked as a professor. His professional interest is now mainly in computer simulation of power electronic circuits and automated computer measuring.